Journal of Marine Science and Technology

Volume 23 | Issue 5 Article 13

NUMERICAL CRASHWORTHINESS ANALYSIS OF AN OFFSHORE WIND TURBINE JACKET IMPACTED BY A SHIP

Hervé Le Sourne
GeM Institute, UMR 6183 CNRS, ICAM Nantes, Carquefou, France., herve.lesourne@icam.fr

Andres Barrera
EMSHIP Master student, ICAM Nantes, Carquefou, France.

Jose Babu Maliakel
EMSHIP Master student, ICAM Nantes, Carquefou, France.

NUMERICAL CRASHWORTHINESS ANALYSIS OF AN OFFSHORE WIND TURBINE JACKET IMPACTED BY A SHIP

Acknowledgements

The authors would like to thank the region “Pays de la Loire” for its financial support but also STX France and Bureau Veritas for their technical participation in defining the scope of this work. It is also worth noting that the work presented in this paper has been performed in the framework of EMSHIP Erasmus Mundus Master (www.EMHIP.EU).

Journal of Marine Science and Technology, Vol. 23, No. 5, pp. 694-704 (2015)
DOI: 10.6119/JMST-015-0529-1

NUMERICAL CRASHWORTHINESS ANALYSIS OF AN OFFSHORE WIND TURBINE JACKET IMPACTED BY A SHIP

Hervé Le Sourne[1], Andres Barrera[2], and Jose Babu Maliakel[2]

Key words: ship collision; offshore wind turbine jacket; nonlinear finite element analysis; structural crashworthiness.

ABSTRACT

The objective of the present work is to understand the crushing behavior of a predefined wind turbine jacket when it is impacted by a ship. To investigate the resulting deformation modes and the repartition of dissipated energy, nonlinear finite element analyses are performed to simulate both rigid and deformable ships colliding the jacket at different velocities. In a first part, a sensitivity analysis to the jacket impacted area is carried out to find the most damaging situation. Then, the influences of gravity loads, wind force, and soil stiffness are studied, considering that the striking ship is rigid. In a second part, the jacket is supposed to be collided by two different deformable vessels and the internal energy distribution between the jacket and the striking ships is analyzed for different jacket leg thicknesses. Some numerical analyses focus also on the transfer of the crushing force between the impacted leg to the others through the braces. All these numerical results will further serve to fix the hypotheses for the development of a simplified tool based on analytical formulations.

I. INTRODUCTION

Ever since the first offshore structures were installed in the Gulf of Mexico at the beginning of the last century, the collision with passing and operating ships has been a major concern to guarantee the safety and operational durability of the structures. For this reason, continuous research is being carried out in this field to characterize the collision and failure procedure of the offshore structures and the impacting vessels, to reduce the risk of potential collision, mitigate structural and environmental damage and prevent the loss of life and overall resources.

Paper submitted 06/16/14; revised 01/31/15; accepted 05/29/15. Author for correspondence: Hervé Le Sourne (e-mail: herve.lesourne@icam.fr).
[1] GeM Institute, UMR 6183 CNRS, ICAM Nantes, Carquefou, France.
[2] EMSHIP Master student, ICAM Nantes, Carquefou, France.

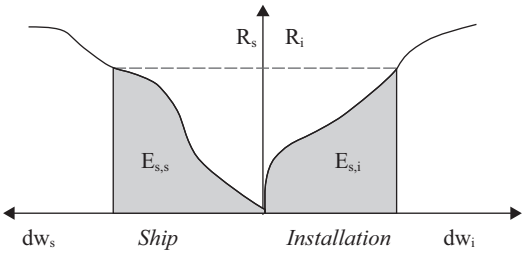

Fig. 1. Collision of an OSV against an offshore structure: resistance *vs.* penetration curves (Ohtsubo, 1995).

1. Numerical Approach

As no experimental or accidental results are available, finite element analysis is an efficient approach to understand the behavior of such structure in case of collision. In the branch of numerical simulations, various models have been developed to simulate the crushing process and to assess the damage of wind turbine supporting structures (pillars, jackets…) or offshore platforms when they are impacted by a vessel.

Visser (2004) established that to assess the resistance of components of fixed platforms, the manners in which energy is dissipated include:

- Local denting
- Elastic beam bending
- Plastic bending/hinge formation
- Plastic tensile strain
- Global deflection of the installation
- Local deformation of the ship

These damage modes are commonly used throughout the literature to characterize the failure behavior of offshore beam structures using numerical, analytical and experimental approaches.

Numerical ship-jacket collision analyses also include the work presented by Amdahl and Johansen (2001), where force *vs.* penetration curves were obtained colliding a 2500 ton Offshore Supply Vessel (OSV) at 2 m/s against an offshore platform pillar. The curves presented in Fig. 1 have been implemented into the NORSOK N-004 Standard (2004) and

can be advantageously used to estimate the deformation of either the jacket or the striking ship from the initial kinetic energy of the ship. The area under the curve gives the energy absorbed through the deformation of the striking ship and the jacket structure.

Grewal and Lee (2004) attempted to estimate the amount of energy that a jacket structure can absorb by plastic deformation during a collision before collapse occurs, and its "reserve strength" after an impact compared to environmental loads (weight, waves, winds, etc.). The ABAQUS finite element code was employed to simulate the effects of a ship impact on different jacket structures using springs to model the soil/structure interaction.

Biehl (2005) used the non-linear finite element code LS-DYNA to study different offshore wind turbine support structures (monopile, jacket and tripod) impacted by single and double hull tankers and cargo ships. The effects of gravity and the loads due to the motion of the turbine were first initialized with an implicit calculation, followed by an explicit calculation to simulate the collision. The interaction of the soil was also considered by modelling it with solid elements and by using an adapted behavior law.

More recently, Vredeveldt and Schipperen (2013) presented an elasto-plastic analysis of an offshore structure impacted by various cargo ships. The developed numerical model accounted for the rupture of some braces or legs using an erosive law based on a shear criteria. This structure supports gas or oil lines and the objective of this study was to estimate the jacket critical damage beyond which the line becomes unusable.

2. Simplified Approaches

The drawback of the numerical approach is that the modelling effort is often quite important, as both the ship and the collided structure have to be finely meshed. Such approach is also time-expensive and consequently not convenient at the beginning of the design process, when the final properties of the structure are not completely fixed. Moreover, in the framework of a full collision risk analysis where different striking vessels and different collision scenarios have to be considered, a simplified analytical approach allowing for a rapid approximation of the jacket crashworthiness becomes more relevant.

The analytical techniques developed to study vessel impacts on jacket structures are very similar to those developed for the study of ships collisions. Several authors like Furnes (1980), Amdahl (1983), Wierzbicki and Hoo Fatt (1993), Hoo Fatt et al. (1996) and Zeinoddini et al. (1998) have derived explicit formulas for the resistance force of a cylinder impacted by a mass as a function of deformation. The structural local dynamic effects are always neglected and the local deformation of the cylinder and its overall bending around plastic hinges is estimated analytically and compared to drop test results.

Semi-empirical methods include the pioneer work presented by Minorsky (1959) who established a correlation between the internal energy and the damage volume of the crushed ships based on statistical data. Simplified analytical solutions for ship collision and grounding analyses include the work of Hong and Amdahl (2008), who assessed the crushing resistance and local denting of web girders under localized loads.

Research work has also been performed to study the crushing resistance of impacted stiffened panels and simplified methodologies have been carried out by Otsubo (1995) and Wierzbicki (1995) to calculate the crushing resistance of metal plates.

These analytical expressions have allowed for the development of analytical or semi-analytical tools that are more or less used for industrial applications. One of the most used codes in offshore industry is the USFOS program which permits to estimate the damage of collided offshore welded tube structure (Amdahl and Eberg, 1993) taking into account the coupling between non-impacted and impacted cylinders. Among the hypotheses adopted when developing such simplified tools, the legs and braces constituting the installations are often supposed to be locally impacted (the shape of the striking ship bow is not considered) and the obliqueness of the cylinders axes with respect to the direction of impact is not taken into account.

The crushing process of a leg or a brace impacted by a ship bow has already been recently studied in details by Buldgen et al. (2014). Considering an oblique ship impact against a cylinder clamped at its extremities and taking into account the geometry of the stern or the bulb, they developed analytical formulations useful to calculate the cylinder crushing force as a function of the penetration.

3. Objectives of the Present Work

The work presented in this paper lies within the framework of the CHARGEOL research project led by STX France and Bureau Veritas and funded by the French region of "Pays de la Loire". The "collision" work package aims first to understand the crushing behavior of a jacket supporting structure with help of finite element simulations. Then, from a better knowledge of the involved deformation modes in legs and braces, analytical formulations will be derived and implemented in a simplified tool, for use during the predesign stage of offshore wind turbine jackets. As no experimental results are yet available, results from finite element simulations will also serve to validate the analytical formulations.

At the beginning of the project, several questions arose regarding the boundary conditions and load cases to consider for the F.E. calculation, regarding the collision scenarios to simulate (initial velocity, impact point, collision angle…) and more generally regarding the jacket or the tower deformation modes. First, taking for example a typical OSV as striking ship, it is interesting to know the more damaging impact scenario between a brace joint impact and a leg collision. The second work aims to understand whether the effects of gravity and soil stiffness have to be considered throughout the

Table 1. Jacket and OSV particulars.

Jacket Particulars		Jacket F.E. model	
Height (m)	63.7	Nb of elts	299198
Width (m)	18	Nb of nodes	241200
Waterline (m)	34	Elt size (m)	0.1
Weight (tons)	540	Elt Type	B-T shell[1]
Legs: ext diam./thick.	24	Material	S355 steel
Braces: ext diam/thick.	30		

OSV Particulars	
Length (m)	102.4
Breadth (m)	23.23
Depth (m)	25.89
Draft (m)	4.117
Disp. (tons)	5000
Water added Mass (tons)	250

[1] *Reduced Integrated Belytchko-Tsai shell elements* (Hallquist, 2013).

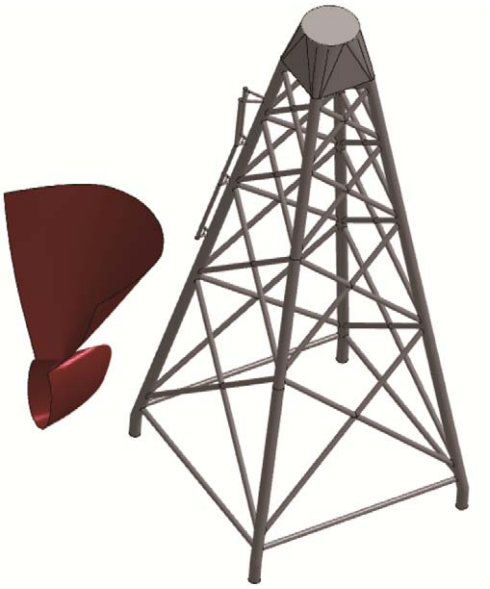

Fig. 2. Jacket and OSV bow finite element models.

deformation process of the jacket. Third, the understanding of the behavior of the wind turbine tower and its effect on the collided jacket is required, as well as the study of the contribution of the non-impacted braces and legs regarding the overall energy dissipation.

All the above sensitivity analyses can be performed considering a rigid striking ship but in reality, the crushing mechanism of the striking vessel absorbs a part of the initial kinetic energy. Therefore, several numerical simulations considering deformable striking vessels are also carried out with the objective to investigate both the repartition of the dissipated energy between the ship and the jacket and its sensitivity to the jacket leg thickness.

II. COLLISION ANALYSIS OF A RIGID SHIP WITH A DEFORMABLE OFFSHORE WIND TURBINE JACKET

1. Model Description

The particulars of the jacket and OSV models used for the calculations are illustrated in Table 1, while Fig. 2 presents a view of finite elements models used for the simulations.

The primary goal of this section is to analyze the crushing behavior of the jacket when it is impacted by an OSV bow. As a conservative approach for evaluating the jacket's resistance, the striking vessel is supposed to be rigid and the soil stiffness is assumed to be infinite so the four jacket leg extremities are affected to clamped boundary conditions.

In order to model the behavior of the S355 steel constituting the structure, a piece-wise linear isotropic hardening material law (Hallquist, 2013) is adopted without considering the strain rate effect as done by Amdahl and Johansen (2001).

The possible rupture of some jacket components is accounted for by using an erosive law based on a shear criteria. The associated threshold failure strain is calculated according to Lehmann and Peschmann (2002)

$$\varepsilon_f = \varepsilon_g + \varepsilon_e \frac{t}{l_e}$$

where ε_f is the failure strain, ε_g the uniform strain, ε_e the necking strain and where t/l_e is the thickness/element size ratio.

2. Comparison of Two Impact Scenarios

To determine the critical impact location with the jacket's design waterline, a scenario where the OSV bow impacts the jacket on one leg is compared to the case of a brace joint impact. Vertical position of impact point accounts for striking ship and jacket draught. In both simulations, an initial impact velocity of 6 m/s is considered as it leads to an initial kinetic energy sufficient for damaging the jacket. Because of the OSV's geometry, the impact occurs both in the stem and bulb areas for both leg and brace scenarios in the same order (first contact at the stem, followed by the bulb).

As the leg impact scenario is concerned, the total crushing force and energy dissipated by plastic deformation of the legs are shown in Fig. 3. The impacted leg dissipates approximately 60% of total internal energy, the rear leg around 15% while the rest is dissipated through deformation of the other legs. After a penetration of 3.65 m, the striking vessel stops and the crushing force drops down to zero.

Fig. 4 shows the plastic strain distribution in the jacket, the red color denoting a plastic strain equal or greater than 1%. It appears that plastic strain develops not only in the impacted area but also in the rear leg through punching of the connected braces. Moreover, plastic hinges develop in all legs extremities near the mudline.

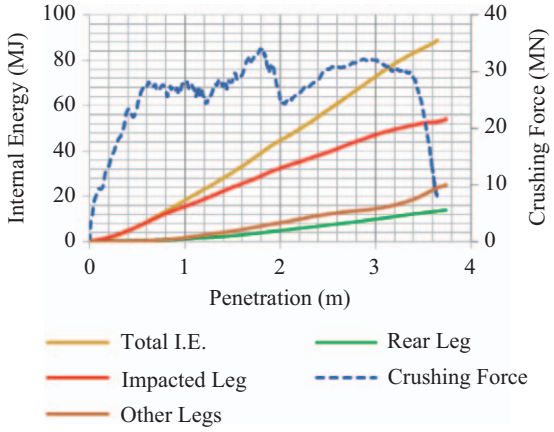

Fig. 3. Leg collision-Internal energies & crushing force.

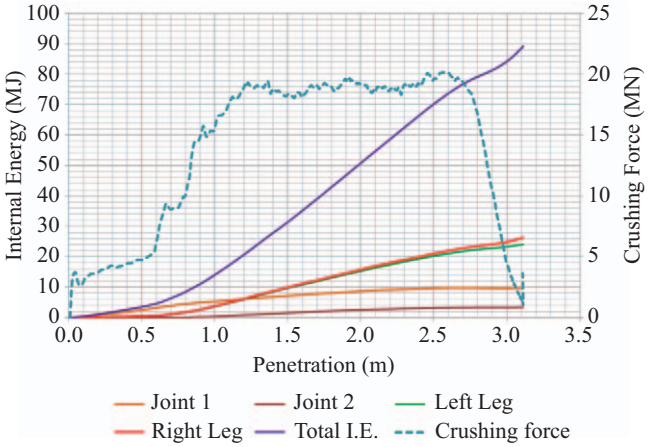

Fig. 5. Braces joint collision-Internal energies & crushing force.

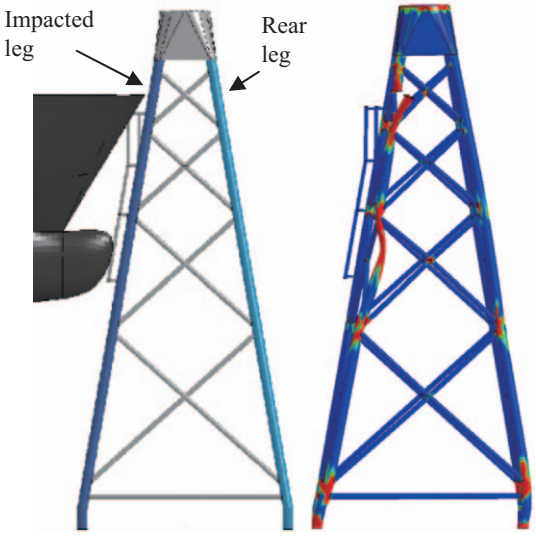

Fig. 4. Leg collision-Plastic strain contours at the end of the collision (red means > 1%).

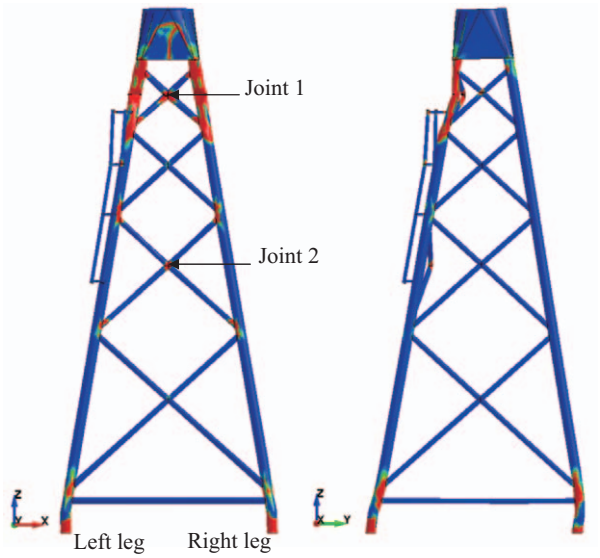

Fig. 6. Braces joint collision-Plastic strain contours after 0.5 s (red means > 1%).

As the brace impact scenario is concerned, internal energies shown on Fig. 4 are calculated for the entire brace joint (all 4 braces that make up a joint).This scenario reflects a more evenly distributed internal energy, since impact occurs in two legs and several braces. The two impacted legs dissipate approximately 30% of strain energy each, the other legs 25%, the remaining 15% being dissipated by the braces.

The geometry of the OSV does not permit the complete rupture of the braces because contact with the legs occurs before initiation of rupture. However, considerable plastic strain develops in the impacted sections, with several finite elements deleted both in legs and brace joint at the height of the stem.

For this last scenario, the penetration does not exceed 3.11 m, as compared to the penetration of 3.65 m observed in the leg collision scenario.

Comparing the jacket damages depicted in Figs. 4 and 6, it is observed that an impact on a leg causes its total rupture while a brace joint collision does not cause full rupture of the legs, even if a great amount of straining is localized near the impact point. All these results show that considering the same striking ship and the same impact velocity, a leg impact seems to be more harmful to the jacket's structure. This scenario is therefore chosen to characterize the influence of gravity loads, to assess the effects of the OWT tower and to study the crushing force transfer via the non-impacted braces through the overall jacket.

3. Sensitivity Analysis to Gravity Loads

To assess the sensitivity of the jacket behavior to the weight of the wind turbine, a two-step LS-DYNA implicit/explicit simulation is carried out, as shown by the flowchart depicted in Fig. 7. Collisions simulations are performed for initial striking ship velocities of 2 and 6 m/s, assuming right angle impacts between the vessel and the jacket. The 2 m/s velocity

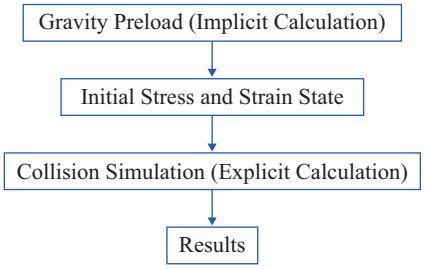

Fig. 7. Simulation flow chart.

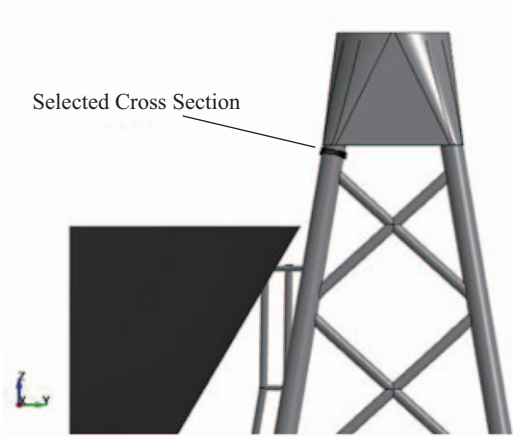

Fig. 8. Post-processed cross section.

is the typical in-service velocity of OSV navigating in a wind turbine field and 6 m/s velocity is chosen to create sufficient indentation of jacket.

The compressive load supported by each leg is analytically estimated to be equal to 1.57 MN, considering the wind turbine weight (573 tons) and the transition piece weight (66 tons) equally distributed on the four legs. The LS-DYNA simulation leads to a compression load of 1.627 MN (3.6% error), noting that this force has been post-processed on the selected cross section illustrated in Fig. 8. Whatever is the impact velocity, it is observed that the plastic strains, crushing force and internal energy do not present noticeable variations.

Concretely, with regards to the crushing forces depicted on Fig. 9, the collided leg crushing force presents a maximum variation of 4% and 2% for the 2 and 6 m/s cases respectively. On the other hand, the maximum internal energy of the structure varied from 3% to 1.3% for the 2 and 6 m/s cases respectively and as expected, the contours of plastic strain throughout the structure are almost identical for both cases. It can therefore be established that when studying the crushing behavior of such a jacket, the gravity effects are not considerable enough in the deformation stage so as to be considered in an analytical approach. It should be also noticed that this only holds true for the time step of the crushing process, as it is clear that for a collapse analysis of the overall wind turbine (including the support) the gravity should be considered.

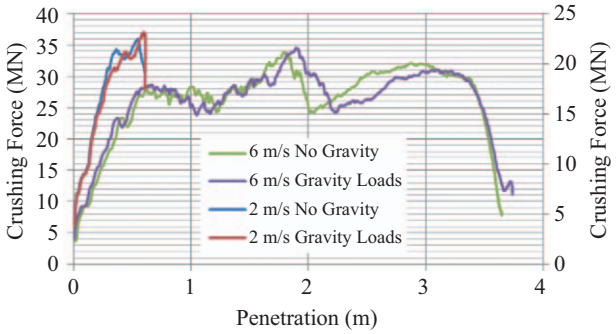

Fig. 9. Comparison of the crushing forces obtained with and without gravity loads.

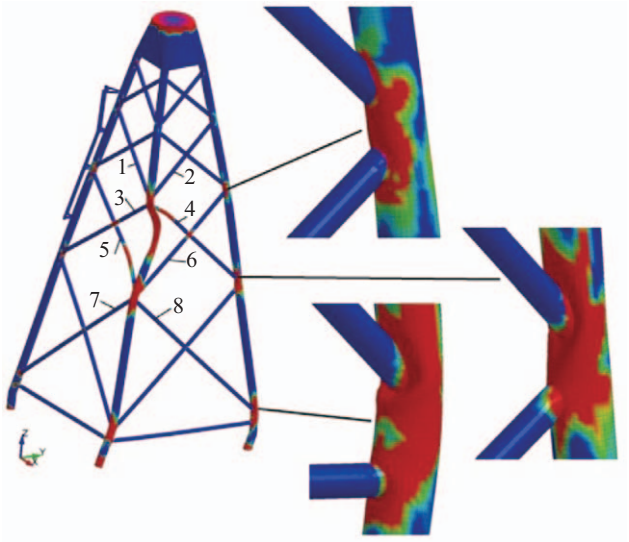

Fig. 10. Effective plastic strain-Punching on rear leg (red means > 1%).

4. Analysis of the Crushing Force Transfer through the Jacket

A study of the force transfer from the impacted leg section to the non-impacted braces is also carried out with the objective to quantify the loads which cause serious punching and plastic deformation of the non-impacted legs (Fig. 10).

For each of the 8 braces studied, labeled 1 to 8 on Fig. 10, the resultant force is post-processed at two probe points, i.e. at the joint with the impacted leg and at the joint with the opposite leg, in order to establish whether the joints between braces affect the resultant force transfer process. Moreover, the simulation is configured so that only the bulbous bow impacts perpendicularly the structure at a 6 m/s initial velocity. This "worst case scenario" leads to a maximum penetration of 4.8 m without rupture of the leg section. The time step at which the maximum crushing force occurs for the impacted leg is isolated and the corresponding transferred resultant forces throughout the non-impacted braces are presented in Table 2.

Fig. 10 presents the contours of plastic strain and shows that during the collision, the impact force transfers through braces

Table 2. Resultant of transferred forces in bent braces (white) and compressed braces (grey).

Brace	Resultant Force (MN)	
	Impacted leg	Opposite leg
1	8.7	8.2
2	5.4	4.0
3	3.3	3.2
4	17.6	17.3
5	6.2	4.6
6	9	4.2
7	9.0	6.2
8	3.8	3.0

2, 4, 6 and 8, which "pierce" the rear right leg. The load transfer also produces the buckling of brace 4 and plastic bending of braces 1, 3, 5 and 7.

Analyzing the values listed in Table 2, it is observed that about 93% of the compressive force is transmitted through the upper node via braces 2 and 4 to the rear leg. However, as the lower node is concerned, only 58% of the compressive force is transmitted via braces 6 and 8 to the rear leg. Anyway, it is difficult to extract from these results a simple rule giving the repartition of the transferred crushing force via the braces to the rear leg and this question needs to be further investigated.

5. Analysis of the Wind Turbine and Tower Influence

So far, only the jacket has been explicitly modelled, the rest of the structure (tower and wind turbine) being represented by a punctual mass connected to the center of the transition piece.

The wind turbine tower is now explicitly modeled using shell elements and the loads and moments exerted by the rotating turbine are introduced in the model in order to study their influence on the crushing behavior of the jacket structure. The wind turbine is described by its mass and inertia momentum associated with a rigid part fixed at the top of the tower. The platform is idealized as a set of rigid beams spawning from the center of the transition piece and the tower is meshed directly with the transition piece joining the tower to the jacket.

As done for the gravity load sensitivity analysis, a two steps implicit/explicit calculation is run and the total crushing force as well as the jacket components internal energies are post-processed. A local plastic straining appears at the junction of the tower with the transition piece (see Fig. 12). This straining dissipates less than 5% of the total internal energy, as shown in Fig. 11 where the internal energies dissipated by the different jacket components have been compared.

The striking ship penetration grows up to 3.85 m, very close to the 3.65 m penetration obtained from the reference simulation. More generally, comparing with the case without tower, we may conclude that up to the point of maximum penetration, the results do not vary noticeably when modeling the tower and considering the dynamic loads exerted by the wind turbine.

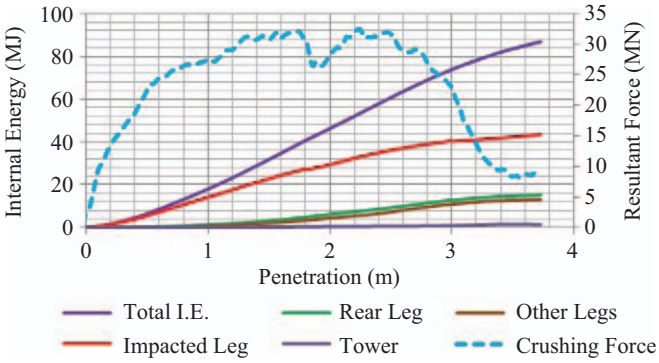

Fig. 11. Model with gravity and tower: Internal energy & crushing force.

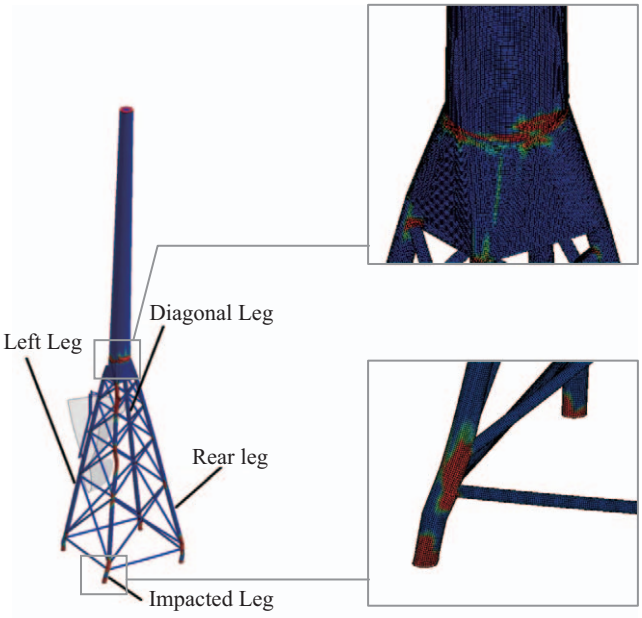

Fig. 12. Jacket plastic strain contours (red means > 1%).

Regarding the tower dynamics, it is interesting to note that the maximum overall displacement at its top reaches 7.3 m (see Fig. 13). Moreover, a detailed analysis of the jacket plastic strain contours reveals that even though the plastic strain distribution is similar to the previous case, a stronger shearing is observed on the legs near the mudline, causing a higher number of elements to fail and finally complete rupture of the impacted leg. As the legs have been conservatively assumed to be clamped at the mudline level, it becomes necessary to study the influence of the soil stiffness on the jacket behavior, knowing that the soil rigidity is actually not infinite.

6. Sensitivity Analysis to the Soil Stiffness

The jacket legs are thrust into the soil approximately 40 m. The previous model including the wind turbine tower is re-used and the flexibility of the soil is accounted for by defining an equivalent soil stiffness related to the mudline level. This stiffness is modelled using translational and rotational

Table 3. Soil stiffness matrix values.

K_{xx}, K_{yy} (MN/m)	$7.4\ 10^3$
K_{zz} (MN/m)	$1.5\ 10^3$
θ_{xx}, θ_{yy} (MN*m/rad)	$1.3\ 10^4$
θ_{zz} (MN*m/rad)	$3.2\ 10^2$

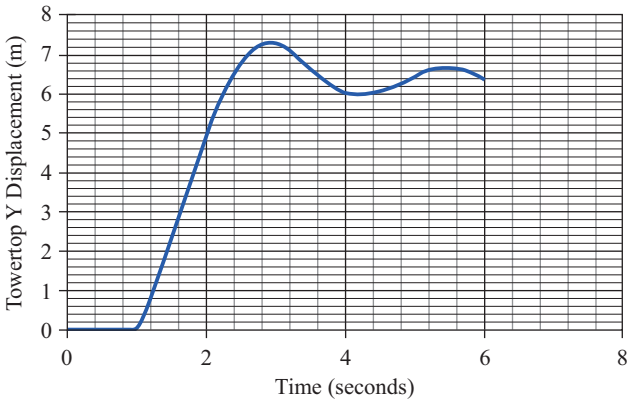

Fig. 13. Time history of tower top displacement.

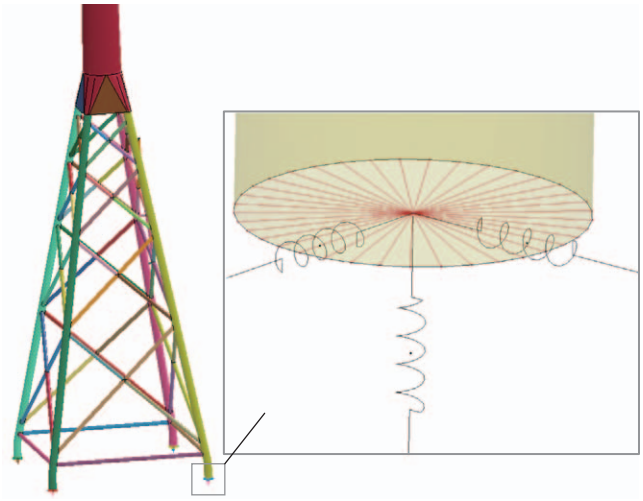

Fig. 14. Rotational and translational springs for soil stiffness.

spring elements connected to the legs extremities as illustrated by Fig. 14. The springs stiffness values defined in Table 3 have been assessed from in-situ geological soil sampling and soil sample stiffness measurements. The post-processed time history of the jacket crushing resistance at the end of the two step implicit/explicit calculation is compared to the rigid soil case crushing force in Fig. 15.

It appears that the soil flexibility characterized by the values listed in Table 3 does not change the jacket legs behavior considerably near the mudline. In fact, the movement of the spring connection point located on the impacted leg is limited to a very small vertical displacement of around 2 cm.

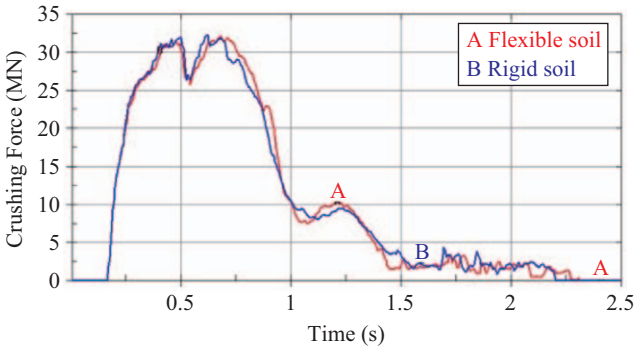

Fig. 15. Comparison of the jacket crushing forces obtained using rigid and flexible soil models.

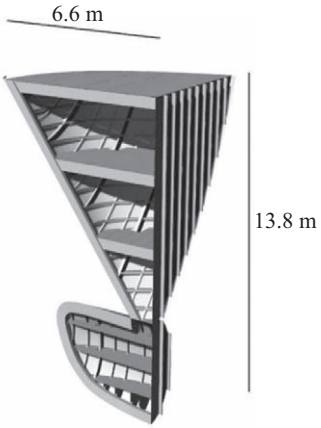

Fig. 16. OSV Bow Geometry.

III. COLLISION STUDY OF TWO DEFORMABLE SHIPS WITH A DEFORMABLE JACKET

1. Deformable OSV Bow Impact Analysis

The bow of a 3000 ton OSV depicted in Fig. 16 is now considered for the deformable ship/jacket collision analysis and its main characteristics are given in Tables 4 and 5. The bow geometry model is a simplified one in the sense that only main structural components are considered (some details have been intentionally ignored). The bow geometry is finely meshed using 100 mm length B-T shell elements associated with a bi-linear elastic-plastic behavior law whose properties are listed in Table 6. The strain rate sensitivity, that is the change in the yield stress at high strain rate $\dot{\varepsilon}$, is calculated according to the Cowper-Symonds relation:

$$1+\left(\frac{\dot{\varepsilon}}{C}\right)^{\frac{1}{p}}$$

where C and p are the strain rate parameters also given in Table 6. A rigid body is associated with the aft part of the bow model in order to represent the rest of the ship.

Table 4. Particulars of the modelled OSV bow.

Length (m)	6.6
Breadth (m)	12
Height (m)	13.8
Frame Spacing (m)	0.6
Double Bottom Height (m)	1.4
Bottom Plating Thickness (mm)	12
Frames	L 180*90*10
Shell Stringers	T 300*100*10
Deck Girders	T 450*150*15
Central Girder	T 500*150*12.5
Bulkhead Stiffeners	L 175*50*12

Table 5. OSV ship particulars.

Length (m)	78
Depth (m)	13.8
Breadth (m)	17.6
Double Bottom Height (m)	1.4
Displacement (T)	3000

Table 6. Material properties of OSV bow structure.

Young's Modulus (MPa)	210000
Yield Strength (MPa)	275
Tangent Modulus (MPa)	3250
Density (Kg/m^3)	7850
Poisson's Ratio	0.3
Strain Rate Parameter, C	40.4
Strain Rate Parameter, p	5

One of the jacket legs is collided by the OSV bow at 43 m above the mudline. An impact velocity of 2.675 m/s is considered to result in an overall collision energy of 11.2 MJ.

Different LS-DYNA simulations are then performed for varying jacket leg thicknesses. The resulting crushing force/penetration curves for both striking ship and struck jacket are compared in Fig. 17. As expected, the jacket structure crushing resistance increases with increasing leg thickness - an important increase is by the way observed from 40 to 50 mm - while the OSV bow crushing behavior does not differ sensitively.

As far as the 40 mm jacket leg is considered, around 75% of the initial kinetic energy is dissipated by crushing of the OSV bow and only 15% by deformation of the jacket, while the remaining part is dissipated by sliding. Moreover, around 75% of the jacket deformation energy is absorbed by the impacted leg itself and only 25% by the rest of the structure. This corresponds to a relatively high susceptibility of the jacket to local deformation.

As far as the 60 mm jacket leg is concerned, the jacket deformation absorbs only 5% of the ship kinetic energy while more than 85% is dissipated by ship crushing. In this case, the impacted leg only absorbs 50% of the jacket deformation energy, 50% being dissipated by the other legs and braces.

Table 7. Internal energy distribution among the OSV structural members.

Structural members	Absorbed energy (%)
Deck plates	30
Deck stiffeners	24
Center girder	20
Hull shell	15
Shell longitudinals	13
Frames	2
Web frames	1

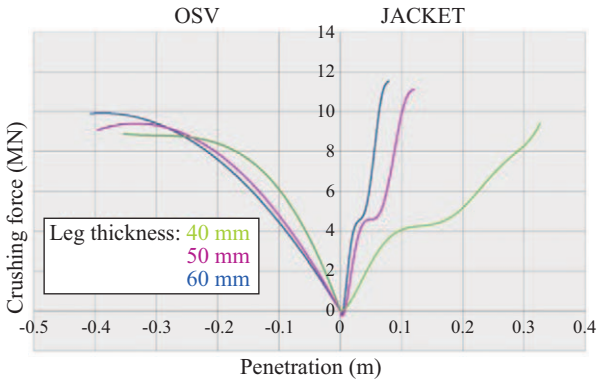

Fig. 17. Force/Penetration curves for varying jacket legs thicknesses.

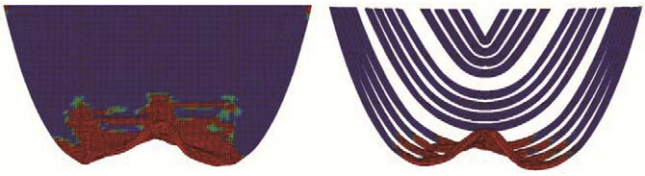

Fig. 18. Effective plastic strain contours of OSV main deck and side stiffeners (red means > 1%).

Whatever is the leg thickness, it is observed that the overall jacket deforms also elastically and tries to come back to its original position after impact. Indeed, a quick energy balance analysis shows that the elastic part of the crushing energy released by the structure is relatively quite important and should therefore not be ignored when developing analytical formulations. On contrary, the elastic part of the OSV bow deformation energy remains negligible.

The energy distribution among the different ship structural members is shown in Table 7. It is worth noting that this distribution is valid only for this particular collision scenario, where the first contact occurs between the hull shell and jacket leg at level of the forecastle deck. As a consequence, the deck plate and associated deck stiffeners play a big role in dissipating the impact energy, as shown in Fig. 18.

Table 8. Bulk carrier particulars.

Length, OA (m)	225
Depth, MLD (m)	20
Breadth, MLD (m)	32.25
Double bottom height (m)	1.7
Draft, scantling (m)	14.15

Table 9. Particulars of bulk carrier cargo hold.

Length (m)	25.65
Breadth (m)	32.25
Height (m)	20
Frame Spacing (m)	0.85
Double Bottom Height (m)	1.7
Bottom Plating Thickness (mm)	20
Frames	T 550*225*15.5
Topside Tank Longitudinals	T 450*180*12.5
Hopper Tank Longitudinals	T 410*125*13 L 300* 90*13 L 350*100*13
Double Bottom Long. Girder	PL 15
Double Bottom Transv. Girder	PL 13

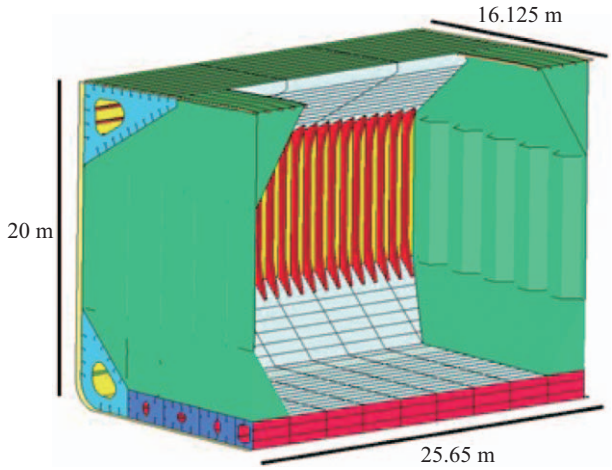

Fig. 19. Bulk carrier hold geometry.

2. Deformable Bulk Carrier Hold Impact Analysis

An 'Ice class IC' panama bulk carrier is now considered to study the case of a drifting ship impacting the jacket along its side. As done for the OSV bow collision study, only the main components of the bulk carrier cargo hold structure depicted in Fig. 19 are considered (small details like brackets are ignored), while Tables 8 and 9 give the main characteristics of the bulk carrier and its cargo hold.

The cargo hold structure is meshed using around 137000 shell B-T elements, similar to those used for modeling the OSV bow (Fig. 20). A rigid body is again defined using all the nodes localized along the hold transverse edges and associated with an inertia matrix which represents the non-modelled part of the bulk carrier. The properties used for defining the elastic-plastic and Cowper-Symonds laws are listed in Table 10.

Table 10. Material properties of bulk carrier.

Young's Modulus (MPa)	210000
Yield Strength (MPa)	355
Tangent Modulus (MPa)	3460
Density (kg/m^3)	7850
Poisson's Ratio	0.3
Strain Rate Parameter, C	40.4
Strain Rate Parameter, P	5

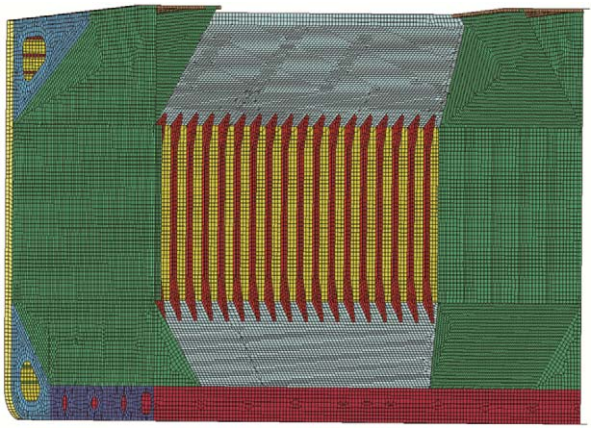

Fig. 20. FE Mesh of bulk carrier hold.

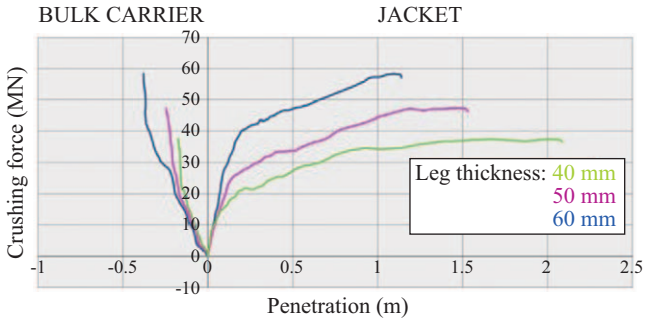

Fig. 21. Force/displacement curves for bulk carrier side Impact.

The bulk carrier cargo is supposed to drift toward the jacket and collide it at 21 m above the mudline with a drifting initial velocity of 1 m/s, and corresponds to an overall collision energy of about 62 MJ. The location of the striking ship side is chosen so as to collide simultaneously two legs. Analyzing the resulting force/displacement curves depicted in Fig. 21, it is observed that when the legs thickness is increased, the strength of the jacket increases as well. However, unlike the observations made for the OSV collision case, it is now the jacket which absorbs the main part of the kinetic energy. This is due to the higher rigidity of the cargo hold stiffening system.

Table 11. Energy dissipation characteristics-ship structural members.

Structural members	Absorbed energy %
Hull shell	44
Hopper tank longitudinals	30
Web frames	24
Other structural members	2

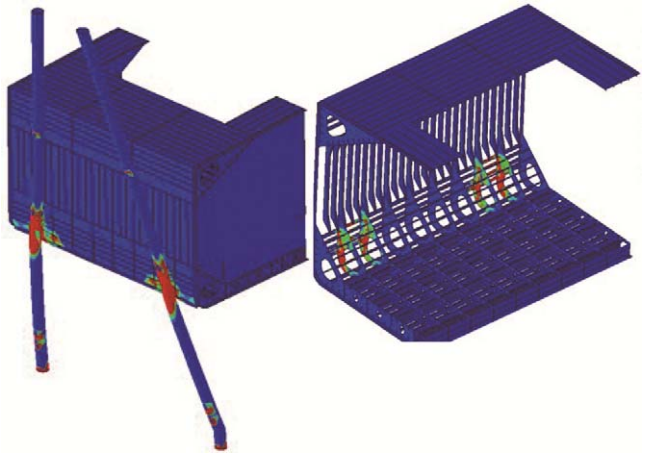

Fig. 22. Plastic strain contours of ship & jacket (red means > 1%).

The distribution of the plastic strain for both the jacket and the striking ship side is plotted on Fig. 22. It is observed that plastic hinges develop in both impacted legs not only around the impact area but also near the mudline.

Regarding the internal energy distribution, even for the largest leg thickness (60 mm), the jacket dissipates up to 80% of the initial kinetic energy while the ship absorbs only 14%. For the lowest leg thickness (40 mm), the jacket dissipates around 90% of the energy and the vessel only 4%. In this last case, it is clear that considering the striking ship as rigid would be acceptable when using a simplified analysis method.

The absorbed energy distribution among the ship structural members is shown in Table 11. The first contact point is at the hull shell plate outside the hopper tank. It appears that the absorbed energy is quite equally distributed between the hull shell, the hopper tank longitudinals and the web frames.

To conclude this section, it is worth noting that energy distribution between the jacket and the striking ship depends largely on the overall stiffness of the colliding area. Whatever is the studied striking ships, the collision scenarios considered in this study involve local impacts on the jacket. Even if the cargo hold strikes two legs simultaneously, the jacket crushed areas remain small and in the same order than the jacket area crushed by the OSV bow.

In fact, the main difference between both studied striking ships is the stiffness of the impacting area. The hold of the bulk carrier is so stiff near the impact point that mostly all the energy is dissipated by the jacket deformation. At contrary, the OSV bow looks much more flexible and absorbs by deformation the main part of the initial kinetic energy.

IV. CONCLUSION

Extensive nonlinear numerical simulations have been carried out to analyze the behavior of a wind turbine jacket when it is collided by a ship.

Firstly, considering that the jacket is collided by a rigid Offshore Supply Vessel, it was determined that an impact against a leg is more detrimental than a collision directed towards a brace joint. It was also shown that accounting the gravity pre-load does not affect the jacket crushing behavior considerably. As a consequence, it will not be necessary to account for it in the initial development of a simplified calculation tool. Finally, taking into account the loads applied by the wind turbine and considering the deformation of the tower was not a noticeable variation in the crushing response of the jacket.

A force transfer analysis also revealed that the legs (primary supporting members) are more susceptible to localize deformation than the non-impacted braces are to buckling. This observation is useful to identify the different deforming modes which have to be accounted for when developing simplified formulations. However, the distribution of the impact forces through the braces was not clearly identified and further investigation must be done in order to know more precisely which part of the crushing force is transmitted through the braces to the rear legs.

Supposing that the pillars are clamped in a rigid soil, plastic hinges were observed on the jacket near the mudline, leading in some particular cases to the rupture of the impacted leg. The soil flexibility was therefore modelled using translational and rotational springs but the resulting behavior of the jacket did not change noticeably. This results proves that given a typical sea ground stiffness, the ‘clamped leg’ hypothesis is acceptable.

When a deformable striking OSV bow was considered for the collision simulations, it was observed that the striking bow absorbs the majority of the energy, even when the leg thickness is varied between 40 and 60 mm. Since the first point of impact was the upper deck, the deck plate, associated stiffeners and the central girder dissipated a majority of the strain energy. Looking at the energy dissipation characteristics, it was also concluded that considering a rigid OSV striking bow would be far too conservative.

In case of ‘Ice Class 1C Panamax’ bulk carrier side impact, the numerical simulation showed that the strength of the jacket also increases with increase in leg thickness. However, the energy dissipation characteristics of the bulk carrier side impact scenario was also looked into and it was found that it is the jacket that absorbs in this case the majority of the energy, whatever the jacket leg thickness is. Since the first point of impact was the hull shell plate outside the hopper tank, a majority of the energy was dissipated by the hull shell plate,

the hopper longitudinal stiffeners and web frames. From these results, it can be said that a simplification considering a rigid striking ship would be acceptable.

The results obtained from this numerical work were helpful to visualize quite precisely the deformation modes of the jacket for different impact scenarios. They will now be used to fix the hypotheses and orient the developments of an analytical tool based on a super-element approach.

ACKNOWLEDGMENTS

The authors would like to thank the region "Pays de la Loire" for its financial support but also STX France and Bureau Veritas for their technical participation in defining the scope of this work. It is also worth noting that the work presented in this paper has been performed in the framework of EMSHIP Erasmus Mundus Master (www.EMHIP.EU).

REFERENCES

Amdahl, J. (1983). Energy Absorption in Ship-Platform Impacts. PhD Thesis. Norway Technological Institute.

Amdahl, J. and E. Eberg (1993). Ship collisions with offshore structures. International Conference on Structural Dynamics (EURODYN), Rotterdam, The Netherlands.

Amdahl, J. and A. Johansen (2001). High Energy ship collision with jacket legs. 11th International offshore and Polar Engineering Conference, Stavanger, Norway.

Biehl, F. (2005). Collision safety analysis of offshore wind turbines. LS-DYNA Anwenderforum, Bramberg, Germany.

Buldgen, L., H. Le Sourne and T. Pire (2014). Extension of the super-element method to the analysis of a jacket impacted by a ship. Marine Structures 38, 44-71.

Furnes, O. and J. Amdahl (1980). Ship collisions with offshore platforms. Intermaritec Conference, Trondheim, Norway.

Grewal, G. and M. Lee (2004). Strength of minimum structure platforms under ship impact. Journal of Offshore Mechanics & Arctic Engineering 126.

Hallquist, J. O. (2013). LS-DYNA User's Manuals Version 971(1) & (2).

Hong, L. and J. Amdahl (2008). Crushing resistance of web girders in ship collision and grounding. Marine Structures 21, 374-401.

Hoo Fatt, M. S., T. Wierzbicki, M. Moussouros and J. Koenig (1996). Rigid plastic approximations for predicting plastic deformation of cylinder shells subject to dynamic loading. Journal of Shock & Vibration 3, 169-181.

Le Sourne, H., N. Besnard, C. Cheylan and N. Buannic (2012). A ship collision analysis program based on upper bound solutions and coupled with a large rotational ship movement analysis tool. Journal of Applied Mathematics 2012.

Lehmann, E. and J. Peschmann (2002). Energy absorption by the steel structure of ships in the event of collisions. Marine Structures 15.

Lützen, M., B. C. Simonsen and P. T. Pedersen (2000). Rapid prediction of damage to struck and striking vessels in a collision even. International Conference of Ship Structure for the New Millennium: Supporting Quality in Shipbuilding, Arlington, USA.

Minorsky, V. (1959). An analysis of ship collisions with reference to protection of nuclear power plants. Journal of Ship Research 3, 1-4.

Ohtsubo, H. and G. Wang (1995). An upper-bound solution to the problem of plate tearing. Journal of Marine Science and Technology 1, 46-51.

Pedersen, P. T. and S. Zhang (1998). On impact mechanics in ship collisions. Marine Structures 11, 429-449.

Standards Norway (2004). NORSOK STANDARD N-004: Design of steel structures. Standards Norway.

Visser, P. (2004). Ship collision and capacity of brace members of fixed steel offshore platforms. Health and Safety Executive, U.K.

Vredeveldt, A. W. and J. H. A. Schipperen (2013). Safe jacket configurations to resist boat impact. Collision and Grounding Ships Offshore Structures, Trondheim, Norway.

Wierzbicki, T. (1995). Concertina tearing of metal plates. Int. J. of Solids Structures (32), 2923-2943.

Wierzbicki, T. and M. S. Hoo Fatt (1993). Damage assessment of cylinders due to impact and explosive loading. Int. J. of Impact Engineering 13, 215-241.

Zeinoddini, M., J. E. Harding and G. A. R. Parke (1998). Effect of impact damage on the capacity of tubular steel members of offshore structures. Marine Structures 11, 141-157.